Predissociation of HCN/DCN in Two Lowest-Lying Singlet Excited States: Effect of Fermi Resonances on Spectra and Dynamics

Dingguo Xu,[†,‡] Daiqian Xie,[‡,§] and Hua Guo*[,†]

Department of Chemistry, University of New Mexico, Albuquerque, New Mexico 87131, Department of Chemistry, Sichuan University, Chengdu, Sichuan, P. R. China, and Institute of Theoretical and Computational Chemistry, Department of Chemistry, Nanjing University, Nanjing 210093, P. R. China

Received: June 18, 2002; In Final Form: August 21, 2002

The three-dimensional potential energy surfaces of the $1^1A''$ and $2^1A'$ states and the corresponding transition dipole surfaces from the ground electronic ($1^1A'$) state of HCN have been obtained from high-level ab initio calculations. Using these surfaces, we investigate the predissociation dynamics of HCN and DCN with a recursive quantum mechanical method. Whereas the perpendicular transition to the $1^1A''$ state leads to narrow predissociative resonances, the absorption spectrum of the parallel $2^1A' \leftarrow 1^1A'$ transition is dominated by relatively broad peaks associated with rapid fragmentation. Detailed analysis suggests that the $1^1A''$ spectrum of DCN is affected by a 1:2 Fermi resonance between the C−N stretching and bending modes. Both theoretical and experimental evidence suggests that the so-called β band should be reassigned to the $1^1A''$ absorption. In the $2^1A'$ state, a strong isotopic effect is found in the fragment internal state distribution and attributed to a Fermi resonance between the H−C and C−N vibrational modes.

I. Introduction

The first thorough investigation of the absorption spectrum of HCN and DCN was reported by Herzberg and Innes nearly fifty years ago.[1] The spectrum starts at ∼52 300 cm^{-1} with a series of weak but well-resolved vibrational features that were collectively labeled as the α band. From rotational analysis, these authors attributed the α band to a transition from the linear ground electronic ($\tilde{X}^1\Sigma^+$ or $1^1A'$) state to an excited $^1A''$ state. The vibrational progressions were assigned to bending overtones and combinations with one quantum in the CN mode. The extensive bending excitation in the absorption spectrum indicates a nonlinear excited state. The equilibrium geometry of the $1^1A''$ state was determined to be $R_{CH} = 1.143$ Å, $R_{CN} = 1.296$ Å, and $\gamma = 125°$, on the basis of rotational analysis of the ground vibrational state. At higher energies, the absorption peaks become increasingly broad. The resolution of rotational structure is no longer possible above ∼55 900 cm^{-1}. The diffuseness of the peaks stems from predissociation, which results in the cleavage of the H−CN bond.

The absorption of the deuterated isotopomer (DCN) in the same spectral range is more complex. In addition to the α band, some features above ∼56 800 cm^{-1} could not be fitted to the Dunham expression without producing some "unreasonable" anharmonicity constants. Herzberg and Innes thus decided to label them as the β band.[1] The upper electronic state was believed to be still of a $^1A''$ character because of the absence of $\Delta K = 0$ features in the spectrum. Consequently, these authors postulated that a second and higher $^1A''$ state must exist in this spectral range. It is interesting to note that the peaks in the DCN absorption are much sharper than those of HCN in the same region, reflecting slower predissociation. Above ∼57 200 cm^{-1}, the peaks do become completely diffuse.

The assignment of the α band to the $1^1A'' \leftarrow 1^1A'(^1\Sigma^+)$ transition has since been confirmed by numerous ab initio calculations.[2−7] The $1^1A''$ state derives from a $^1\Sigma^-$ state in linearity. Its equilibrium geometry and fundamental frequencies from ab initio calculations are in good agreement with experimental observations.[6,8−10] For example, Botschwina et al.[8] have obtained the equilibrium geometry of the $1^1A''$ state ($R_{CH} = 1.143$ Å, $R_{CN} = 1.296$ Å, $\gamma = 125°$), which is very close to the experimental data. Recent dynamical calculations based on three-dimensional potential energy surfaces (PESs) also yielded semiquantitative agreement with experiment concerning the position and lifetime of the predissociative resonances.[9−12] Internal state distributions of the CN fragment from low-lying predissociative resonances on the $1^1A''$ PES have also been calculated by us.[10]

The assignment of the β band, on the other hand, has remained a subject of controversy. The existence of another $^1A''$ state in the vicinity of $1^1A''$ was challenged by theoretical studies of the excited-state PESs.[2,5] These ab initio calculations found that the $2^1A''$ (derived from a $^1\Delta$ state at linearity) state lies significantly above the onset of the β band and has a linear minimum. Consequently, it could not possibly be responsible for the β band absorption. Some theoreticians speculated that the $2^1A'$ state might serve as an alternative candidate for the $\beta \leftarrow \tilde{X}$ spectrum, on the basis of the positions and intensities of vibrational features calculated from one-dimensional potentials cuts.[2,5−7]

The questions raised by the theoretical studies prompted additional isotopic measurements and a reassignment of the β band by Innes and co-workers.[13−15] These authors argued that the absence of the $\Delta K = 0$ bands precludes a possible $^1A'$ assignment and suggested that the β band be fitted to a bending progression associated with the first C−D overtone in the $1^1A''$ state. Unfortunately, the C−D harmonic frequency (ω_1) extracted from the fitting (2455 cm^{-1}) is significantly larger than that obtained from a recent high-level ab initio study (1921

[†] University of New Mexico.
[‡] Sichuan University.
[§] Nanjing University.

10.1021/jp021442v CCC: $22.00
Published on Web 10/08/2002

cm^{-1}),[8] which led Botschwina et al. to reject the new vibrational assignment. This theoretical value of ω_1 is supported by several later ab initio studies.[7,12] So far, no consensus has been reached regarding the nature of the upper electronic state responsible for the β band of DCN.

In addition to the absorption spectra, there have been some interesting fluorescence studies in the α band.[16,17] It was found that the lowest-lying ro-vibrational features in the α band have uncharacteristically shorter lifetimes than some of their counterparts at higher energies. The abnormality was attributed to efficient predissociation via interstate crossing or internal conversion to the ground or low-lying triplet states. The fluorescence experiments agree with a later photodissociation study, which detected only $CN(\tilde{X}^2\Sigma^+)$ fragments at a photon wavelength of 193 nm at the red wing of the α band.[18] At higher energies, the predissociation is known to yield $CN(A^2\Pi)$ and H.[19−23] This is consistent with the fact that both the $1^1A''$ and $2^1A'$ states of HCN correlate adiabatically to the $CN(A^2\Pi)$ and H asymptote. The ro-vibrational distribution of the CN fragment has been measured at a number of photon wavelengths.

In this work, we address the controversy about the electronic character of the β band of DCN. We first note that the original rationale for assigning the β band to another $^1A''$ state is not quite convincing because difficulties in fitting the vibrational levels to a Dunham expansion can originate from a number of factors such as the unusually large anharmonicity near a barrier and/or Fermi resonances. On the other hand, it is hard to argue against the strong experimental evidence, namely the absence of $\Delta K = 0$ bands in the rotational fine structure that identified the $^1A''$ character of the upper state. The theoretical assignment of the β band to the $2^1A' \leftarrow \tilde{X}^1\Sigma$ transition fails to reconcile with the experimentally observed $\Delta K \neq 0$ propensity. As shown in this work, it was misled by the intensity calculations carried out on one-dimensional cuts of the excited PES. To unequivocally resolve the issue, one needs three-dimensional potential energy and transition dipole surfaces of both the $1^1A''$ and $2^1A'$ states. Although several detailed studies of the $1^1A''$ state PES have been published,[8−12] neither global potential energy nor transition dipole surfaces of the higher $2^1A'$ state have been reported. As one of the objectives of this work, we present three-dimensional potential energy and transition dipole surfaces based on high level ab initio calculations. We also characterize the nuclear dynamics on both excited electronic states using an efficient recursive quantum mechanical method. This work is organized as follows: The next section (section II) outlines the theoretical method used to calculate the total and partial cross-sections for the photodissociation. Section III discusses the ab initio calculation of the potential energy and transition dipole surfaces. Section IV presents the absorption spectra for both excited states, obtained using the Chebyshev propagation. On the basis of the spectra, we argue that the β band of DCN should be reassigned to a series of vibrational features in the $1^1A''$ state. The calculated internal state distribution of the CN fragment is also presented in the section. Finally, the results are summarized in section V.

II. Theory

The Hamiltonian with zero total angular momentum ($J = 0$) is given below in Jacobi coordinates ($\hbar = 1$)

$$\hat{H} = -\frac{1}{2\mu_R}\frac{\partial^2}{\partial R^2} - \frac{1}{2\mu_r}\frac{\partial^2}{\partial r^2} + \left(\frac{1}{2\mu_R R^2} + \frac{1}{2\mu_r r^2}\right)\hat{j}^2 + V(R,r,\theta) \tag{1}$$

where r, R, and θ are respectively the C−N distance, the distance from the H atom to the center of mass of the CN fragment, and the Jacobi angle, $\hat{j}$ is the CN angular momentum operator, and μ_R and μ_r are the appropriate reduced masses. V is the excited-state PES.

In our previous work,[10] we have used a Lanczos based method[24] to compute the partial and total photodissociation cross-sections in the $1^1A''$ state of HCN and DCN. The Lanczos method is ideally suited for such systems because their spectra are dominated by narrow resonances. However, the convergence becomes difficult if broad resonances are present. In this work, we use an alternative recursive method based on the Chebyshev propagator, which is capable of handling both broad and narrow resonances.

The Chebyshev method is based on the expansion of analytical functions using Chebyshev polynomials of the Hamiltonian:[25−31]

$$F(\hat{H}) = \sum_{k=0}^{\infty} a_k T_k(\hat{H}) \tag{2}$$

where $\hat{H}$ is assumed to have been scaled to $[-1, 1]$. An interesting prospective of the above expansion is in order if one recognizes that the Chebyshev polynomial is a cosine function in disguise: $T_k(x) \equiv \cos(k \arccos x)$. As a result, $T_k(\hat{H}) \equiv \cos k\hat{\Theta}$ with $\hat{\Theta} \equiv \arccos \hat{H}$ can be thought of as a cosine-type propagator with the Chebyshev order (k) as the effective time.[32,33] The analogy with the time-energy conjugacy allows straightforward transplant of existing methodologies based on time propagation.[34] A distinct advantage of the Chebyshev propagator is that it can be evaluated exactly using a three-term recursion.

In particular, we note a special case of eq 2 for the spectral density operator in the angle notation:

$$\delta(E - \hat{H}) = \frac{1}{\pi \sin\theta}\sum_{k=0}^{\infty}(2 - \delta_{k0}) \cos k\theta \cos k\hat{\Theta} \tag{3}$$

where $\theta \equiv \arccos E$. Reminiscent of Heller's expression in terms of the time autocorrelation function,[35] the total photodissociation cross-section can be expressed as a cosine Fourier transform of the autocorrelation function in the Chebyshev order domain ($C_k \equiv \langle\Phi_g|T_k(\hat{H})|\Phi_g\rangle$):[36]

$$\sigma(E) \propto \omega\langle\Phi_g|\delta(E - \hat{H})|\Phi_g\rangle = \frac{\omega}{\pi \sin\theta}\sum_{k=0}^{\infty}(2 - \delta_{k0}) \cos k\theta C_k \tag{4}$$

Here, $E = E_i^g + \omega$ with ω as the photon frequency, and Φ_g is the product of the transition dipole moment and a ground-state eigenfunction: $\Phi_g = \mu_{eg}\phi_i^g$ with $\hat{H}_g\phi_i^g = E_i^g\,\phi_i^g$. In practice, the summation in eq 4 is truncated as C_k approaches zero.

The partial cross-section, or the fragment ro-vibrational distribution, can also be expressed as the Fourier transform of Chebyshev cross-correlation functions ($C_k^{vj} \equiv \langle\eta_{vj}^-|T_k(\hat{H})|\Phi_g\rangle$):

$$\Sigma_{vj}(E) \propto \omega\left|\frac{1}{a_{vj}(E)}\langle\eta_{vj}^-|G^+(E - \hat{H})|\Phi_g\rangle\right|^2 = \omega\left|\frac{1}{ia_{vj}(E) \sin\theta}\sum_{k=0}^{\infty}(2 - \delta_{k0})e^{ik\theta}C_k^{vj}\right|^2 \tag{5}$$

where the outgoing wave packet associated with the internal state quanta vj (η_{vj}^-) is placed at the dissociation asymptote with a_{vj} as its amplitude at E.[37,38] Again, the similarity with the time-dependent version[37] is quite apparent.

The correlation functions are computed at every propagation step as overlaps between the propagation state ($\psi_k = T_k(\hat{H})\psi_0$) and prespecified states (Φ_g and η_{vj}^-). In practice, a modified Chebyshev recursion was used in the propagation:[29,30]

$$\psi_{k+1}^d = d(2\hat{H}\psi_k^d - d\psi_{k-1}^d) \qquad k \geq 1 \tag{6}$$

with $\psi_0^d = \Phi_g$ and $\psi_1^d = d\hat{H}\Phi_g$. The damping ($d$) is placed near the edge of the R grid to effectively impose the outgoing wave boundary condition. In this work, we used $d(R) = 2[1 + e^{\alpha}(R - R_d)]^{-1}$ for $R \geq R_d$ and $=1$ everywhere else. It is interesting to note that the Chebyshev propagation can be carried out in real arithmetic.

Although the Chebyshev and Lanczos methods are both based on the Krylov subspace, their convergence characteristics may differ. The Chebyshev method discussed above is essentially a transform method that is inherently restricted by the uncertainty principle. In other words, the energy resolution is inversely proportional to the number of propagation steps. As a result, it is well suited for fast processes such as the photodissociation in the $2^1A'$ state. We note in passing that spectral resolution beyond the uncertainty principle can be achieved using the idea of filter-diagonalization.[39,40] On the other hand, the Lanczos method used in our earlier work[10,24] relies on the complete resolution of the eigenspectrum. For low-lying bound or narrow resonance levels, the Lanczos method typically converges faster than the Chebyshev method even when spectral estimators such as low-storage filter-diagonalization are used.[41,42]

III. Potential Energy and Transition Dipole Surfaces

The PES of the $1^1A''$ state has been discussed in our earlier work,[10,12] so we concentrate here on the PES of the $2^1A'$ state. The adiabatic potential energies were generated by the MOLPRO suite of ab initio programs[43] using the internally contracted multireference configuration method with the Davidson correction (icMRCI+Q).[44] The reference wave functions were taken to be the natural orbitals obtained from the state-averaged CASSCF calculation for the equally weighted $1^1A'$, $1^1A''$, and $2^1A'$ states, including all valence molecular active orbitals (2548 and 2744 CSFs for the $^1A''$ and $^1A'$ symmetries). The transition dipoles are obtained at the CASSCF level. The aug-cc-pVTZ basis set of Dunning[45] was employed, resulting in a total of 115 cGTO. Additional calculations with the aug-cc-pVQZ basis set were performed to ascertain the accuracy of the calculations. The total number of contracted configurations in the MRCI calculations is about 0.9 million, which correspond to about 35 million uncontracted configurations. All calculations were performed in the C_s symmetry framework.

A nonuniform direct product grid in the internal coordinate system was selected for potential energy surfaces: 17 C−H coordinate points from 1.23 to 11.5 (1.23, 1.53, 1.83, 2.03, 2.23, 2.43, 2.63, 2.83, 3.03, 3.23, 3.73, 4.23, 4.73, 5.23, 6.50, 8.50, 11.5) a_0, 9 points for C−N coordinate varied from 1.58 to 3.38 (1.58, 1.98, 2.13, 2.28, 2.38, 2.48, 2.68, 2.88, 3.38) a_0, and 12 points for HCN angle ranged from 40° to 180° (40°, 50°, 60°, 80°, 90°, 100°, 110°, 120°, 130°, 140°, 160°, 180°) were used, which give a total of 1836 points. In the interaction region, the potentials at smaller angles are very high in energy and sometimes difficult to converge. Because of their limited importance in our dynamical calculations, these values were obtained via extrapolation. Finally, a three-dimensional spline interpolation provided values of the potential energy surface between grid points. A similar strategy was used to generate the transition dipole surfaces, but with a much denser grid.

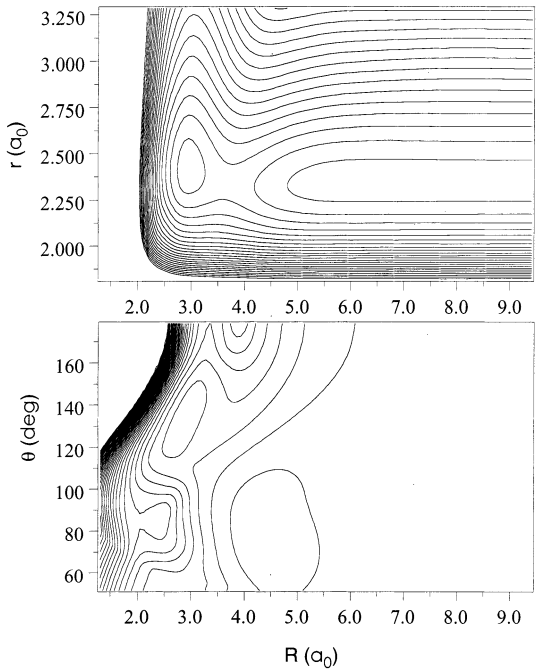

Figure 1. Contour plots of the $2^1A'$ PES of HCN in Jacobi coordinates. Upper and lower panels are cuts of the PES at $\theta = 138°$ and $r = 2.418$ a_0, respectively, which correspond to the HCN minimum. The contour interval is 0.01 hartree.

Figure 1 displays the contour plots of the $2^1A'$ state PES in the Jacobi coordinates. The upper panel shows a barrier in the dissociation coordinate, which is associated with the conical intersection between the $1^1\Pi$ and $1^1\Delta$ states. The saddle point of the barrier nearly coincides in the vibrational coordinate with the equilibrium C−N distance in the fragment, rendering negligible the final state interaction for the vibrational degree of freedom. In fact, the entire potential exhibits rather weak coupling between the vibrational and dissociation coordinates. The overall topology of the $2^1A'$ PES in this plot is similar to that of the $1^1A''$ state, although the latter has a much deeper minimum.

However, the behavior of the $2^1A'$ PES in the bending coordinate is quite different. As shown in the lower panel, the PES is dominated near linearity by the $1^1\Pi/1^1\Delta$ conical intersection. At bent configurations, there are two potential minima. The first one is quite shallow and located at $R_{CH} = 1.130$ Å, $R_{CN} = 1.286$ Å, $\gamma = 114.3°$, corresponding to a bent HCN isomer. Our equilibrium position is close to the previous theoretical result ($R_{CH} = 1.130$ Å, $R_{CN} = 1.297$ Å, $\gamma = 112°$) obtained with a smaller basis set.[6] This minimum is 0.266 eV above the dissociation limit with a barrier height of 0.167 eV. The depth of this well is significantly smaller than that of the $1^1A''$ state (0.625 eV).[10] As a result, it is not expected to support any long-lived resonance states. It is also interesting to note that the saddle point is at $R_{CH} = 1.391$ Å, $R_{CN} = 1.257$ Å, $\gamma = 89.4°$, about 25° away from the equilibrium angle.

The second well corresponds to an HNC isomer and is located at $R_{CH} = 2.477$ Å, $R_{CN} = 1.217$ Å, $\gamma = 60.74°$. Its existence has not been reported before by either ab initio or experimental studies. Interestingly, the HNC minimum is quite deep, 0.771 eV below the HCN minimum and 0.496 eV below the

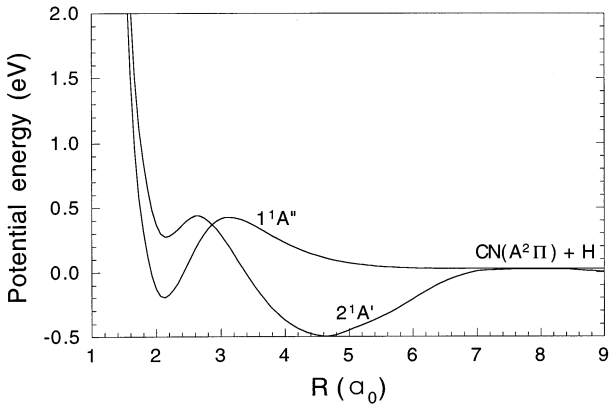

Figure 2. Minimal energy paths of the $2^1A'$ and $1^1A''$ PESs along the dissociation coordinate (R).

dissociation limit. However, the HNC minimum is unlikely to be populated by photoexcitation from the linear ground state. The two minima and the dissociation barrier of the $2^1A'$ PES are more readily seen in Figure 2, in which the minimal energy path along the dissociation coordinate (R) is plotted. For comparison, the minimal energy path of the $1^1A''$ PES is also given in the same figure.

The transition from the ground ($1^1A'$) to $2^1A'$ state is of a parallel nature. The transition dipole has two components in the molecular (yz) plane. In the linear configuration, the $2^1A'$ state has a $^1\Delta$ character at small R_{CH}. The electronic transition from the ground ($^1\Sigma^+$) state is thus forbidden, as characterized by zero transition dipole moments. However, the transition becomes allowed at larger R_{CH} where the $2^1A'$ state assumes a $^1\Pi$ character. For the dissociation at the red-wing of the $2^1A'$ absorption band, excitation near the ground-state equilibrium ($R_{CH} = 1.065$ Å) is nominally forbidden but facilitated by nonzero transition dipole moments in bent configurations. The situation is very similar to the $1^1A''$ state, which is dominated by a $^1\Sigma^-/^1\Pi$ conical intersection. The transition dipole moments near the ground-state equilibrium are shown in Figure 3.

IV. Photodissociation Dynamics

In the numerical calculations, the excited-state Hamiltonian was discretized in a direct product discrete variable representation (DVR) grid.[46] Eighty and thirty sine-DVR[47] points were used to cover the R range [1.7, 9.5] a_0 and the r range [1.8, 3.3] a_0, respectively. A seventy point Gaussian-Legendre DVR grid in the range [0, 180°] was used in the angular coordinate. Although a much smaller grid suffices for the absorption spectrum, this large grid is needed for the final state projection. In the Chebyshev propagation, the Hamiltonian is scaled to [−1, 1]: $\hat{H}_{scale} = (\hat{H} - H^+)/H^-$ with $H^\pm = (H_{max} \pm H_{min})/2$. The damping was switched on at $R_d = 8.3\ a_0$.

IVA. Absorption Spectra. For comparison, absorption spectra for both the $1^1A''$ and $2^1A'$ states were calculated. The initial state was determined using a real-symmetric Lanczos method on an ab initio based PES of the ground electronic state.[8] Only transitions from the ground vibrational state were considered. Because the overall rotation was ignored in our calculations, the absorption spectrum for the $2^1A' \leftarrow 1^1A'$ transition was approximated by a simple sum of the y and z contributions.

The upper panel of Figure 4 displays the absorption spectra for the $1^1A''$ and $2^1A'$ states of HCN. The energy zero is chosen at the zero-point energy (ZPE) level in the $1^1A''$ state. As shown in the figure, the $1^1A''$ spectrum is dominated by sharp

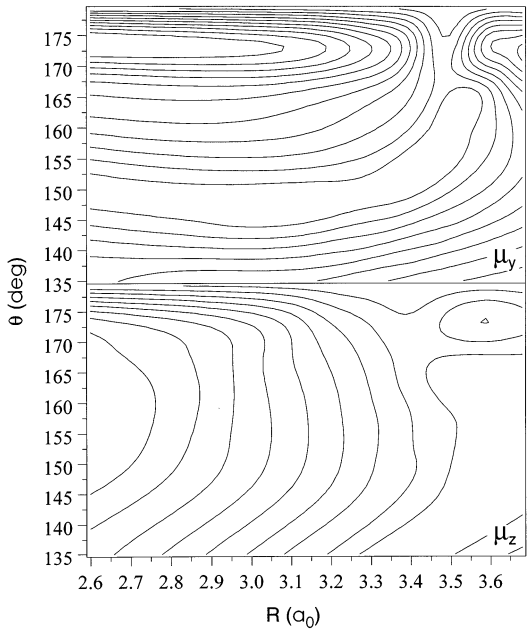

Figure 3. Contour plots of the y- and z-components of the transition dipole in Jacobi coordinates at $r = 2.18\ a_0$, which is the C−N equilibrium of the ground electronic state. The contour interval is 0.03 au.

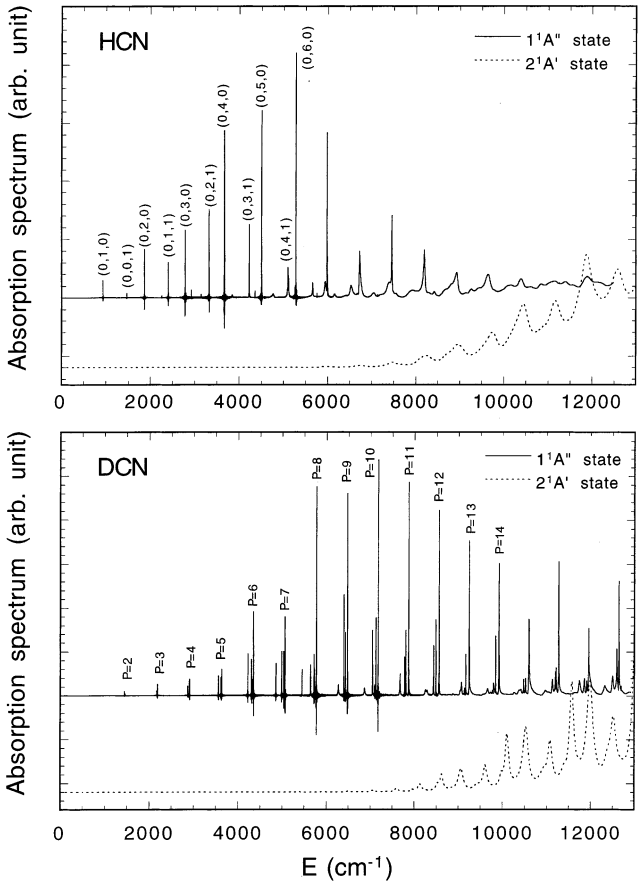

Figure 4. Calculated HCN and DCN absorption spectra for the $1^1A'' \leftarrow 1^1A'$ and $2^1A' \leftarrow 1^1A'$ transitions.

resonances at low energies, in quantitative agreement with our earlier results obtained using a different numerical method,[10,12] and consistent with the experimental observation of Herzberg and Innes.[1] Because of these narrow resonances, the Chebyshev propagation was carried out for 60 000 steps. The resulting spectral resolution is adequate for our discussion here, but still

insufficient to resolve the widths of some low-lying resonances. Assignments of low-lying resonances are given in terms of three vibrational quantum numbers (n_1, n_2, n_3), which correspond to the C−H stretch, H−C−N bend, and C−N stretch, respectively. These assignments reveal the dominance of two bending progressions (0, n_2, 0) and (0, n_2, 1), thanks to the linear-to-bent nature of the transition. Above 6000 cm^{-1}, the width of the vibrational features increases drastically due to strong predissociation. The spectrum in this spectral range was not reported in our earlier work[10] because of convergence problems in the Lanczos propagation.

The $2^1A'$ spectrum of HCN, also shown in Figure 4, consists of a progression of much broader peaks. The widths of these peaks are typically on the order of a few hundred wavenumbers, which corresponds to a lifetime of a few tens of femtoseconds. Such diffuse peaks preclude any rotational resolution. Numerically, a much shorter (∼8000) Chebyshev propagation was sufficient. The lack of sharp peaks in the spectrum is indicative of the fact that the shallow HCN minimum of the $2^1A'$ PES is incapable of supporting any bound or long-lived resonance states.

The much more interesting case of DCN absorption spectra is given in the lower panel of Figure 4. As mentioned in our earlier work,[10] the $1^1A''$ spectrum of DCN is dominated by regularly spaced clusters of spectral peaks, which is in sharp contrast with the HCN spectrum. The inter-cluster separation is approximately 700 cm^{-1}, roughly the bending frequency. Low-lying resonances have been assigned with the three vibrational quantum numbers (n_1, n_2, n_3) in our previous work.[10] From these assignments, it is clear that the spectral pattern is due to the fact that the bending frequency ($\upsilon_2 = 726$ cm^{-1}) is nearly half of the C−N stretching frequency ($\upsilon_3 = 1463$ cm^{-1}). Indeed, we have found evidence of a 2:1 Fermi resonance from the eigenfunctions. In Figure 4, each cluster is hence labeled by the polyad quantum number $P = n_2 + 2n_3$.[48] Interestingly, the experimental spectrum of Herzberg and Innes also has a very similar cluster pattern.[1] As shown in Figure 4, the diffuseness of the peaks generally increases with energy. However, the peak width is substantially narrower than the HCN ones at the nearby energy, signifying slower predissociation. This is consistent with experimental observations[1] and can be attributed to the more massive deuterium.

The $2^1A'$ spectrum of DCN resembles that of HCN in that no sharp peaks are present. Again, the broad resonances can be attributed to the shallow well in the $2^1A'$ state PES. Although their widths are smaller than the corresponding HCN peaks, these resonances are still extremely short-lived with subpicosecond lifetimes.

The broad but well-defined peaks in the $2^1A'$ state absorption spectra of HCN and DCN can be understood as the result of partial recurrence of wave packet on the excited state PES. In Figure 5, trajectories of the excited state wave packets immediately after the transition are displayed in the two radial Jacobi coordinates. Upon excitation, the $2^1A'$ state PES exerts forces in both coordinates that result in the elongation of the C−N and H/D−C bonds. However, the initial motion of the wave packet does not immediately lead to dissociation even though the total energy is above the saddle point of the barrier. Instead, the wave packet is bounced back by the potential barrier and revisits the Franck−Condon region. The recurrence in the DCN autocorrelation function near $k = 250$ is clearly seen in the insert of Figure 5. Subsequently, energy gradually flows from the C−N mode to the R coordinate and the dissociation ensues. This initial recurrence results in a progression of features

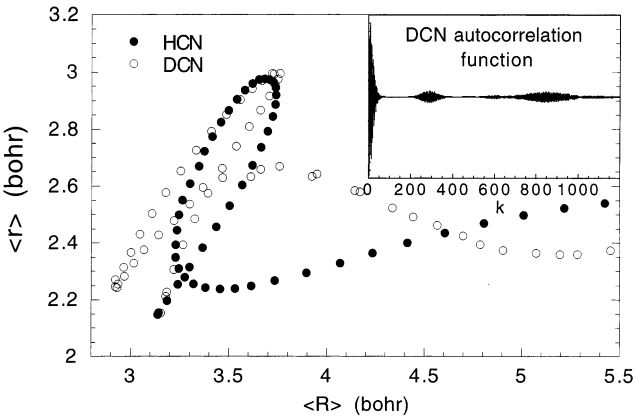

Figure 5. Trajectories of the excited state wave packet immediately after the excitation. The DCN autocorrelation function is given in the inset.

that are separated by roughly 1500 cm^{-1} and assignable to the C−N stretch excitation. In addition to the initial recurrence due to the C−N vibration, there are some subsequent recurrences, as shown in the DCN autocorrelation function displayed in Figure 5. These recurrences occur at longer periods and correspond to the bending vibration. In fact, many (but not all) peaks in Figure 4 are assignable. For instance, the peak at 8623 cm^{-1} in the DCN spectrum can be assigned as (0, 10, 0) and the next two peaks at higher energies (9064 and 9608 cm^{-1}) are (0, 8, 1) and (0, 9, 1), respectively. The assignment of the HCN spectrum is hindered by a strong Fermi resonance between the C−H and C−N stretching modes, as discussed below.

IVB. Assignment of the β Band. It is clear from the DCN spectra in Figure 4 that the $2^1A'$ state could not possibly be responsible for the β band of DCN, which was experimentally known to have well-resolved rotational structures.[1] In a previous theoretical study,[6] Peric et al. concluded on the basis of potential cuts in the three vibrational coordinates that the HCN potential well in the $2^1A'$ state is quite stable. Although our potential cuts at the same coordinates are consistent with their lower-level ab initio results, the global PES paints a quite different picture of its topology in three dimensions. As discussed in section III, the $2^1A'$ state potential well corresponding to the HCN isomer is extremely shallow. Its depth in our PES (0.167 eV) is only about one-third of the value (0.434 eV) reported by Peric et al.[6] This difference could be explained by the fact that the saddle point of the barrier is located at a bending angle ($\gamma \sim 90°$) that is quite far away from the equilibrium angle ($\gamma \sim 114°$) and was not considered by Peric et al.[6,7] Indeed, the absorption spectra obtained with the three-dimensional PES clearly indicate strong predissociation for both the HCN and DCN resonances associated with this well. This result led us to reject the notion that the $2^1A'$ state is responsible for the β band of DCN. Our conclusion is further supported by the experimentally observed $\Delta K \neq 0$ propensity of the β band features, which points to a $^1A''$, rather than a $^1A'$, excited state.[1]

Having excluded the $2^1A'$ state, let us now return to the $1^1A''$ spectrum of DCN for a more thorough analysis. Figure 6 compares the calculated spectrum of three ($P = 6, 8, 10$) polyads with the experimental spectrum of Herzberg and Innes in the same energy ranges. Assignments of the peaks in both spectra are given with the three vibrational quantum numbers. We stress that one should not expect a quantitative theoretical−experimental agreement for two reasons. First, basis set errors and the neglect of higher order excitations in the ab initio calculations can easily cause energy differences on the order of a few tens of wavenumbers. Second, additional differences might exist

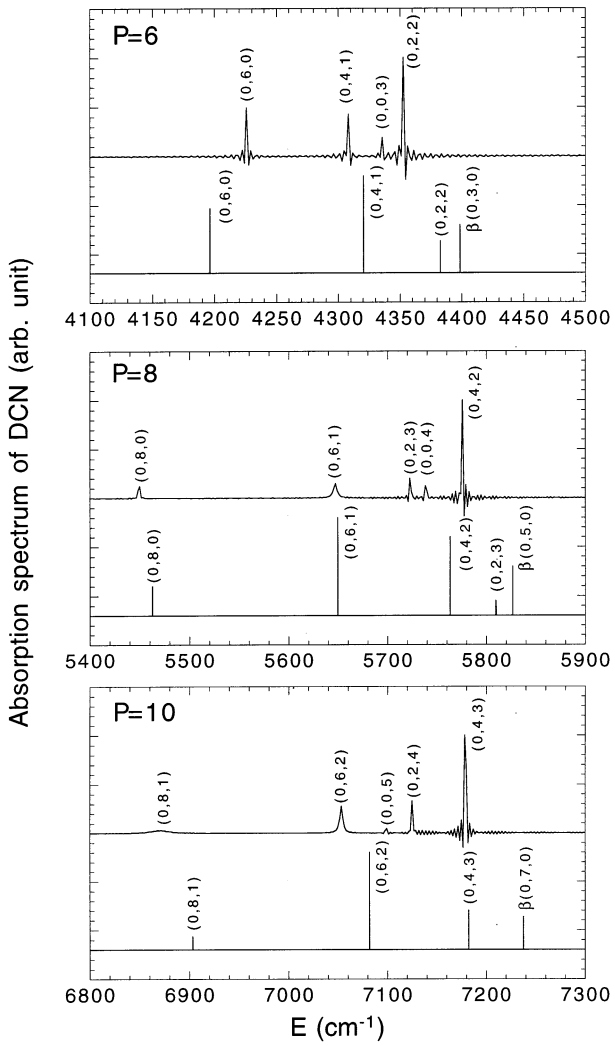

Figure 6. Comparison of the calculated (upper lines) and experimental (lower lines) $1^1A''$ spectrum of DCN for three ($P = 6$, 8, 10) polyads.

because the experimental peaks are for transitions with $\Delta J = 1$. Instead, we look for qualitative patterns shared by the two spectra.

A striking similarity between the theoretical and experimental spectra is that they both have the same number of peaks within each polyad. There are, for example, four and five members for $P = 6$ and 8. In the $P = 10$ polyad, neither theory nor experiment identified the first member of the polyad, namely (0, 10, 0), presumably due to strong predissociation. The (0, 0, 5) level in the theoretical spectrum is very weak and conceivably not observed in the experiment. In addition, there is rather close resemblance in the spectral pattern and relative intensity as well, although it is more difficult to quantify. These observations are also found in other polyads that are not shown in Figure 6. Theoretically, the number of vibrational features in a polyad is determined by the polyad quantum number. For instance, the $P = 6$ polyad consists of the (0, 6, 0), (0, 4, 1), (0, 2, 2) and (0, 0, 3) levels, although some of them might be strongly mixed. Interestingly, Herzberg and Innes made the same assignments of the first three members of this polyad as us, but assigned the last peak to the (0, 3, 0) level of the so-called β band.[1] Similarly, the last peaks in the $P = 8$ and 10 clusters were assigned by these authors as β(0,5,0) and β(0,7,0).[1] The major motivation for their assignment of the β band was the failure in fitting these spectral lines to a single Dunham expansion with "reasonable" anharmonicity constants.[1]

TABLE 1: Fitting Parameters for the Fermi Resonance Hamiltonian (cm^{-1}) for the $1^1A''$ State of DCN

ω_0	51281.33
ω_2	742.22
ω_3	1514.89
x_{22}	3.76
x_{23}	5.54
x_{33}	11.89
y_{222}	−0.2897
y_{223}	−0.1070
y_{233}	0.1876
y_{333}	3.587E−2
k	−2.670
λ_2	−0.1028
λ_3	0.2453
λ_{22}	5.196E−2
λ_{23}	7.326E−2
λ_{33}	−0.1075

We would like to argue that such a conclusion was ill conceived in the first place because of strong anharmonicity near the dissociation barrier and the 2:1 Fermi resonance in DCN. The latter phenomenon is particularly conspicuous in this system but received no mentioning in the original experimental work. To illustrate our point, we have fitted the experimental spectrum, including the features assigned by Herzberg and Innes as the β band, to a spectroscopic Hamiltonian that contains the Fermi resonance term:

$$\langle n_2,n_3|\hat{H}|n_2,n_3\rangle = \omega_0 + \sum_i\left(n_i+\frac{1}{2}\right)\omega_i - \sum_{i\le j}\left(n_i+\frac{1}{2}\right)\times\left(n_j+\frac{1}{2}\right)x_{ij} + \sum_{i\le j\le k}\left(n_i+\frac{1}{2}\right)\left(n_j+\frac{1}{2}\right)\left(n_k+\frac{1}{2}\right)y_{ijk} \quad (7a)$$

$$\langle n_2,n_3|\hat{H}|n_2+2,n_3-1\rangle = \sqrt{n_3(n_2+2)(n_2+1)}\left[k+\lambda_2\left(n_2+\frac{3}{2}\right)+\lambda_3 n_3+\lambda_{22}\left(n_2+\frac{3}{2}\right)^2+\lambda_{23}\left(n_2+\frac{3}{2}\right)n_3+\lambda_{33}{n_3}^2\right] \quad (7b)$$

The fitting involved 23 levels up to 5000 cm^{-1}, including the reassigned β band features. The resulting parameters are listed in Table 1. A reasonable fit (rms = 0.374 cm^{-1}) was found for all the observed levels up to the 11th polyad. If only the diagonal term in eq 7a is used, on the other hand, the fitting is much worse (rms = 1.593 cm^{-1}). Interestingly, the harmonic frequencies in our fitting are in good agreement with the original fitting of Herzberg and Innes[1] (ω_2 = 735.0 cm^{-1}, ω_3 = 1505.8 cm^{-1}) and with previous theoretical results of Botschwina et al.[8] (ω_2 = 756 cm^{-1}, ω_3 = 1505 cm^{-1}).

The results presented above strongly suggest that the so-called β band of DCN should be assigned to the $1^1A'' \leftarrow 1^1A'$ absorption. Our conclusion is based on several pieces of evidence derived from either experimental or theoretical observations. First, the calculated $2^1A' \leftarrow 1^1A'$ absorption spectrum consists of only broad peaks that are inconsistent with the narrow β band features observed in the experiment. Second, the parallel $2^1A' \leftarrow 1^1A'$ transition should produce both $\Delta K = 0$ and ± 1 transitions, but the former was not observed experimentally.[1] Third, the calculated $1^1A''$ spectrum strongly resembles the experimental spectrum in each polyad labeled cluster if the β band features are included. Finally, both the α and β band features in the experimental spectrum can be reasonably fitted to a single spectroscopic Hamiltonian that contains the Fermi coupling. We believe our evidence is sufficiently strong to warrant a reassignment of the so-called β band of DCN.

Although our reassignment agrees with Innes and coworkers[13,15] in that the $1^1A''$ state is responsible for the β band,

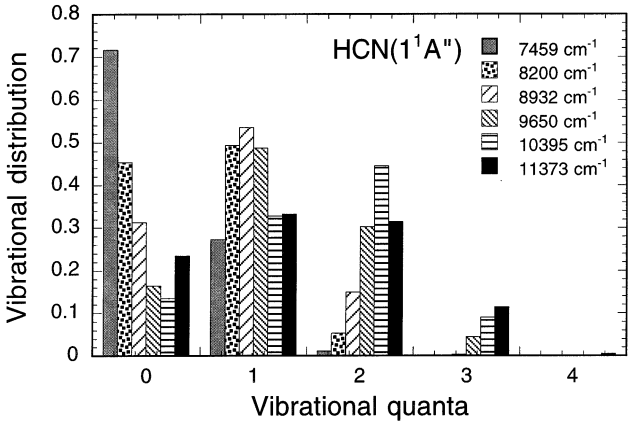

Figure 7. Vibrational distributions of the CN fragment from the HCN photodissociation in the $1^1A''$ state.

the vibrational assignments of these features are different. It is quite certain that the assignment of these features to the D−C overtone excitation by Bickel and Innes[13] is incorrect. In fact, we have found no significant contribution to the DCN absorption spectrum from an excited D−C mode. At this point, however, an unambiguous assignment of the β band features beyond the polyad quantum number is still not possible due to the inaccuracy of the PES.

IVC. Fragment Ro-vibrational Distributions. As discussed in section II, the internal state distribution of the CN($A^2\Pi$) fragment is obtained in this work from Chebyshev cross-correlation functions. The asymptotic wave packet is given as a product of the internal eigenfunction (ϕ_{vj}) and a delta function located at $R_0 = 7.16\ a_0$. In Figure 7, the CN vibrational distribution from the photodissociation of HCN in the $1^1A''$ state is plotted at several energies corresponding to the prominent absorption peaks above 7000 cm^{-1}. In sharp contrast with the resonances at lower energies where only the vibrationless CN are produced,[10] the dissociation of these shorter-lived resonances produces CN fragments with substantial vibrational excitation with v up to 4. Particularly, we note that the CN vibrational distribution at 11 373 cm^{-1}, which corresponds to the 157 nm photon wavelength, is inverted with a peak at $v = 1$. The variation of the vibrational distribution implies some extent of mode specificity. Mode specificity was found in the CN vibrational distribution from the DCN dissociation in the same energy range (not shown here). For both molecules, the vibrational excitation in the CN fragment can be attributed to the excitation of the C−N mode in the parent molecule, as the final-state interaction outside the barrier is rather weak.

The CN vibrational distributions from the $2^1A'$ state photodissociation of both HCN and DCN are displayed in Figure 8 at energies corresponding to the absorption peaks. These distributions reveal an unexpectedly strong isotopic effect. The CN fragment in the HCN dissociation is dominated by the vibrational ground state in the energy range up to 13 000 cm^{-1}, and extensive CN excitation is present in the same energy range for the DCN fragmentation. In fact, the latter CN distribution is inverted at several energies.

Like the $1^1A''$ state, the C−N vibrational mode in the parent molecule can be excited because of the different C−N equilibrium distances in the ground (1.154 Å) and excited (1.279 Å) electronic states. Wave packet motion in the r coordinate, as shown in Figure 5, clearly indicates a significant force in this direction. Given the weak coupling between the vibration and dissociation coordinates in the $2^1A'$ PES shown in the upper panel of Figure 1, it should not be surprising for the CN

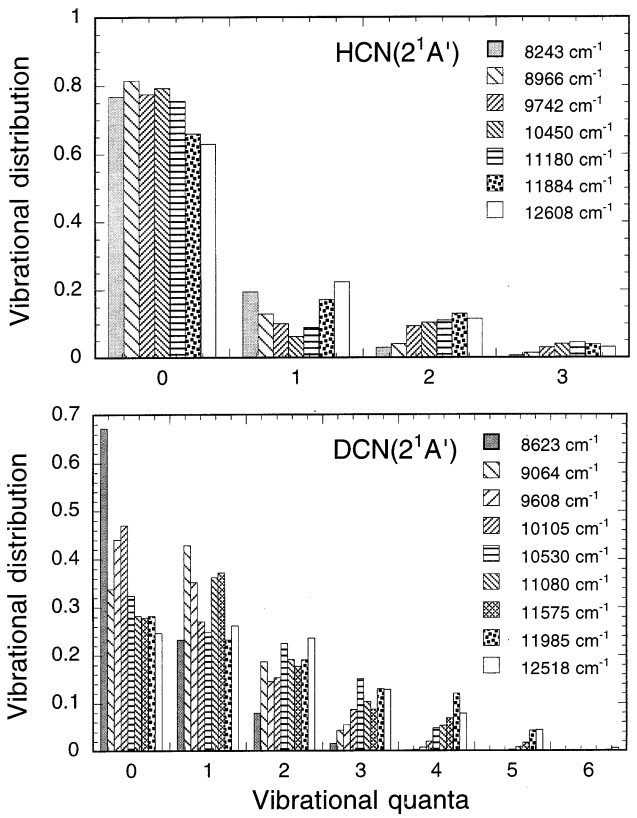

Figure 8. Vibrational distributions of the CN fragment from the HCN and DCN photodissociation in the $2^1A'$ state.

fragment to retain the vibrational excitation in the parent molecule. This argument is indeed borne out for the DCN dissociation. At 8623 cm^{-1}, for example, the (0, 10, 0) resonance produces predominantly $v = 0$ CN fragments. On the other hand, resonances with C−N excitation, such as the one at 9064 cm^{-1}, produce "hotter" CN vibrational distributions.

The uniformly "cold" CN vibrational distribution from the HCN dissociation thus implies efficient dispersion of vibrational energy in the dissociation. This "irregularity" can be attributed the fact that the H−C vibration in the $2^1A'$ state has approximately the same frequency as the C−N vibration (∼1500 cm^{-1}) in the Franck−Condon region. As a result, the two local modes are strongly mixed via a 1:1 Fermi resonance, which results in extremely efficient energy transfer from the C−N vibration to the dissociation coordinate. On the other hand, the D−C vibrational frequency is about 1300 cm^{-1}, which is detuned significantly from the CN vibration and renders inefficient energy transfer. Of course, one should be forewarned that the above analysis is qualitative in nature because the PES in the R coordinate is unbound.

One can identify the aforementioned Fermi resonance by inspecting stationary wave functions $\Phi(E) = G^+(E - \hat{H})\Phi_g$, which were obtained by accumulating the Chebyshev propagation states at energy E. Examples of such L^2-integrable wave functions are plotted in Figure 9. They resemble bound state wave functions inside the barrier near $R \sim 3.5\ a_0$ but possess long dissociation tails at large R. For the DCN wave function, the node in the r coordinate inside the barrier is approximately perpendicular to those in the R coordinate. Thus, it is straightforward to assign this resonance to $n_2 = 1$. The HCN wave function, on the other hand, has an irregular nodal structure that curves around in the two coordinates. Such a curved nodal structure stems from the Fermi resonance between the C−N and H−C modes, which leads to strong mixing between the

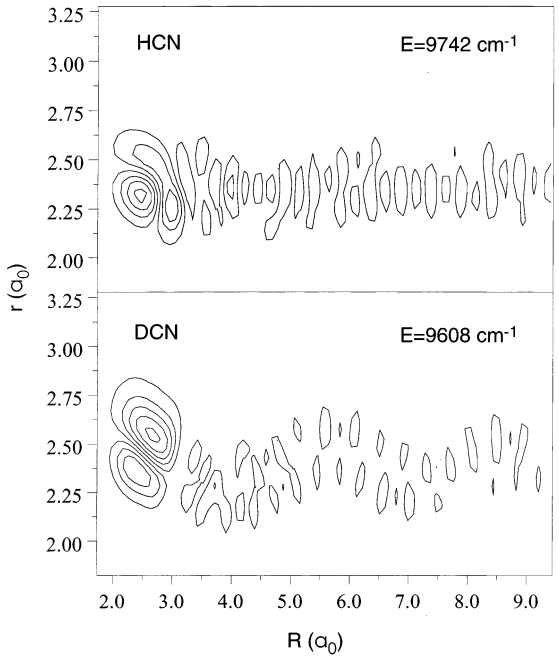

Figure 9. Representative stationary wave functions for HCN and DCN.

two modes and facilitates rapid energy flow to the dissociation coordinate and efficient fragmentation. Indeed, the widths of the HCN absorption peaks are substantially broader than the corresponding DCN ones. In addition, the larger extent of fragment vibrational excitation in the DCN wave function can be clearly seen at large *R*. The pronounced isotopic effect in the CN vibrational distribution is quite striking. It illustrates that Fermi resonances can not only manifest spectroscopically but also affect dynamics.

Experimentally, Guo et al. have measured the vibrational distribution of CN($A^2\Pi$) upon the photodissociation of HCN at 157 nm,[23] which is ~11 373 cm^{-1} in our energy scale. The CN fragment was found to have significant vibrational excitation, but with a small peak at $v = 0$. The theoretical data reported in this work are not inconsistent with the experimental results, if one realizes that at this energy both the parallel and perpendicular transitions contribute. It is thus conceivable that a vibrational distribution with a small peak at the $v = 0$ can result from combining the CN distributions in both Figures 7 and 8. Unfortunately, however, a quantitative comparison with experiment requires calculations with nonzero total angular momenta, which are yet to be carried out. We point out in passing that the theoretical prediction of the electronic-state-resolved CN vibrational distributions can be verified experimentally using polarized lasers in both excitation and detection.

Rotational distributions of the CN fragment at its vibrational ground state are given in Figure 10 for the $2^1A'$ state dissociation. They are all oscillatory and extend to rather large rotational quantum numbers. The extensive rotational excitation in the CN fragment is indicative of the large torque exerted on the CN moiety upon the linear-to-bent transition. The oscillatory structure can be rationalized by the "rotational reflection principle",[49] which attributes the final fragment rotational distribution to the reflection of the bending wave function at the transition state. For example, there are ten minima in the CN rotational distribution from the DCN dissociation at 8623 cm^{-1}, which corresponds to the (0, 10, 0) resonance. Because of the larger bending frequency of the HCN parent, the rotational distribution has in general fewer nodes. Interestingly, the CN rotational distributions from the HCN dissociation are cooler than those from the DCN dissociation, which can presumably be attributed to its faster predissociation rate. At higher vibrational states of the CN fragment, the rotational distribution is typically less excited.

Rotational distributions of the CN fragment at several vibrational levels have been measured by Guo et al. for the 157 nm photodissociation of HCN.[23] Our calculated distributions agree with the experimental results in that both found significant rotational excitation in the CN fragment up to 50 rotational quanta. However, the experimental distributions have peaks around $N = 10-15$ with little oscillation. We believe the discrepancy could be due to the $J \neq 0$ contributions, in addition to the parallel/perpendicular mixing at this wavelength. This speculation has to await further theoretical investigations that include overall rotation of the molecule.

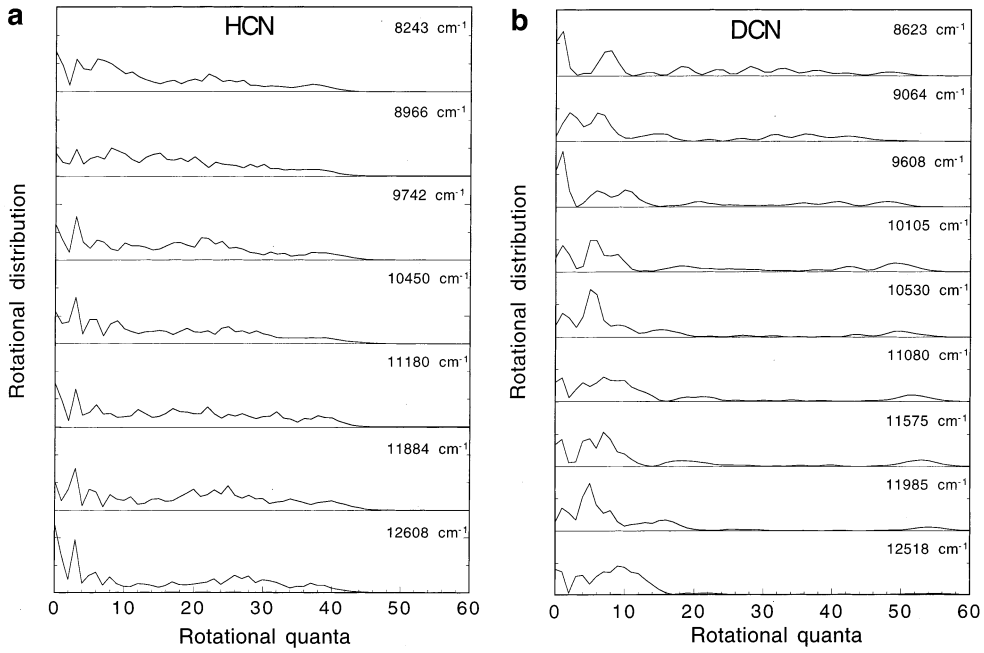

Figure 10. Rotational distributions of the CN fragment in its ground vibrational level upon the HCN and DCN photodissociation in the $2^1A'$ state.

V. Conclusion

A major contribution of this work is the first three-dimensional PES of the $2^1A'$ state of HCN based on high level ab initio calculations. This and the $1^1A''$ state PESs reported earlier[10,12] allowed us to perform accurate dynamical calculations of the HCN and DCN photodissociation in their first absorption band. Useful information, such as absorption spectra, resonance positions and lifetimes, and fragment ro-vibrational state distributions, has been obtained.

In the Franck−Condon region, the $1^1A''$ and $2^1A'$ states arise from the $1^1\Sigma^-$ and $1^1\Delta$ states in linearity, respectively. They form conical intersections with the $1^1\Pi$ state, which correlates to the H/D + CN($A^2\Pi$) asymptotic limit. The remnant of the conical intersection at bent configurations forms an adiabatic barrier in the H−CN coordinate for both the $1^1A''$ and $2^1A'$ states, which is responsible for the predissociative resonances in HCN and DCN. However, the detail topology of the two PESs is quite different. The relatively deep HCN potential well in the $1^1A''$ state PES supports both (adiabatically) bound and long-lived resonance states, whereas the corresponding well of the $2^1A'$ state is so shallow that only short-lived resonances are present. In addition, the $2^1A'$ state possesses a genuinely bound HNC potential well that has never been identified before. Unfortunately, this well is not accessible by Franck−Condon excitation near the linear ground-state equilibrium.

The lifetime of the predissociative resonances are reflected by the width of the absorption peaks, which can be measured experimentally. In the case of the $1^1A''$ state, the low-lying resonances live sufficiently long to resolve their rotational structures. The features in the α band of HCN and DCN can be assigned with vibrational quantum numbers. As shown in our earlier work,[10,12] the calculated positions and lifetimes are in reasonably good agreement with the experimental measurement of Herzberg and Innes.[1] Our calculations reported in this work indicate that the resonances in the $2^1A'$ state are all very broad and not responsible for the narrow absorption peaks observed experimentally.

In particular, we presented strong evidence that the so-called β band in the DCN absorption spectrum is attributable to the $1^1A'' \leftarrow 1^1A'$ transition. Our new assignment is based on the resemblance between our calculated $1^1A''$ spectrum and the experimental one, as well as the lack of long-lived resonances in the $2^1A'$ state. Our theoretical results also suggest that a 2:1 Fermi resonance plays an important role in the DCN spectrum and should be taken into consideration in the assignment. The new assignment of the β band features is further supported by the experimentally observed $\Delta K \neq 1$ propensity. This reassignment resolved a long-standing controversy for this system. We point out that the previous theoretical assignment of the β band to the $2^1A'$ state[6,7] is flawed because of incomplete knowledge of the global $2^1A'$ PES. On the other hand, the experimental assignment to a D−CN overtone progression in the $1^1A''$ state[13] is also erroneous. In fact, our results indicate little excitation in the H/D−CN mode for the $1^1A'' \leftarrow 1^1A'$ transition.

We have also investigated the photodissociation dynamics of both HCN and DCN in the two excited electronic states. In the $1^1A''$ state, the CN vibrational distribution is largely determined by the vibrational quanta of the predissociative resonances. As a result, mode specificity is prevalent in both HCN and DCN. In the $2^1A'$ state, similar predissociation dynamics is found for DCN. However, the HCN dissociation in the $2^1A'$ state is quite different because of the accidental coincidence of the H−C and C−N vibrational frequencies. The 1:1 Fermi resonance promotes efficient energy flow between the two modes, resulting rapid dissociation, and vibrational relaxation. The resulting CN fragment is uniformly dominated by its ground vibrational state. The calculated vibrational distribution of the CN fragment with contributions from the two electronic states is consistent with the experimental measurement at 157 nm.

The CN rotational distribution was found to be highly excited in both electronic states, reflecting the linear-to-bent nature of the transitions. There exists significant mode specificity despite the rapid predissociation in the energy range of interest. The rotational distributions are highly oscillatory, which reflect the highly excited bending wave function in the transition state. A direct comparison with experimental data is not possible at this stage because of the neglect of overall rotation of the parent molecule.

The theoretical investigation of the excited-state dynamics of this simple triatomic system reveals many interesting features the predissociation process. Of particular importance is the influence of Fermi resonances in both spectra and dissociation dynamics, as demonstrated by this study. Given the richness of the dissociation dynamics unraveled by theoretical studies such as this work, we hope more detailed experimental information on this system will be forthcoming.

Acknowledgment. This work was supported by the National Science Foundation (CHE-0090945). Partial support was provided by the Chinese National Natural Science Foundation (20173036) and by the Teaching and Research Award Program for Outstanding Young Teachers in Higher Education Institutions of MOE, PRC.

References and Notes

(1) Herzberg, G.; Innes, K. K. *Can. J. Phys.* **1957**, *35*, 842.
(2) Schwenzer, G. M.; O'Neil, S. V.; Schaefer, H. F.; Baskin, C. P.; Bender, C. F. *J. Chem. Phys.* **1974**, *60*, 2787.
(3) Vazquez, G. J.; Gouyet, H.-F. *Chem. Phys. Lett.* **1978**, *57*, 385.
(4) Vazquez, G. J.; Gouyet, H.-F. *Chem. Phys. Lett.* **1979**, *65*, 515.
(5) Peric, M.; Peyerimhoff, S. D.; Buenker, R. J. *Can. J. Chem.* **1977**, *55*, 3664.
(6) Peric, M.; Dohmann, H.; Peyerimhoff, S. D.; Buenker, R. J. *Z. Phys.* **1987**, *D5*, 65.
(7) Peric, M.; Buenker, R. J.; Peyerimhoff, S. D. *Mol. Phys.* **1988**, *64*, 843.
(8) Botschwina, P.; Horn, M.; Matuschewski, M.; Schick, E.; Sebald, P. *J. Mol. Struct. (THEOCHEM)* **1997**, *400*, 119.
(9) Barbosa, E. S.; McCarroll, R.; Grozdanov, T.; Rosmus, P. *Eur. Phys. J.* **2000**, *D 10*, 225.
(10) Xu, D.; Xie, D.; Guo, H. *J. Chem. Phys.* **2002**, *116*, 10626.
(11) Barbosa, E. S.; McCarroll, R.; Grozdanov, T.; Rosmus, P. *Phys. Chem. Chem. Phys.* **2000**, *2*, 3131.
(12) Xu, D.; Xie, D.; Guo, H. *Chem. Phys. Lett.* **2001**, *345*, 517.
(13) Bickel, G. A.; Innes, K. K. *Can. J. Phys.* **1984**, *62*, 1763.
(14) Meenakshi, A.; Innes, K. K. *J. Chem. Phys.* **1986**, *84*, 6550.
(15) Meenakshi, Innes, K. K.; Bickel, G. A. *Mol. Phys.* **1989**, *68*, 1179.
(16) Hsu, Y.-C.; Smith, M. A.; Wallace, S. C. *Chem. Phys. Lett.* **1984**, *111*, 219.
(17) Jonas, D. M.; Zhao, X.; Yamanouchi, K.; Green, P. G.; Adamson, G. W.; Field, R. W. *J. Chem. Phys.* **1990**, *92*, 3988.
(18) Eng, R.; Carrington, T.; Dugan, C. H.; Filseth, S. V.; Sadowski, C. M. *Chem. Phys.* **1987**, *113*, 119.
(19) Mele, A.; Okabe, H. *J. Chem. Phys.* **1969**, *51*, 4798.
(20) West, G. A.; Berry, M. J. *J. Chem. Phys.* **1974**, *61*, 4700.
(21) Lee, L. C. *J. Chem. Phys.* **1980**, *72*, 6414.
(22) Bucher, C. R.; Lehmann, K. K. *Chem. Phys. Lett.* **1998**, *294*, 173.
(23) Guo, J.; Eng, R.; Carrington, T.; Filseth, S. V. *J. Chem. Phys.* **2000**, *112*, 8904.
(24) Li, S.; Li, G.; Guo, H. *J. Chem. Phys.* **2001**, *115*, 9637.
(25) Tal-Ezer, H.; Kosloff, R. *J. Chem. Phys.* **1984**, *81*, 3967.
(26) Huang, Y.; Zhu, W.; Kouri, D.; Hoffman, D. K. *Chem. Phys. Lett.* **1993**, *214*, 451.
(27) Huang, Y.; Kouri, D. J.; Hoffman, D. K. *Chem. Phys. Lett.* **1994**, *225*, 37.
(28) Zhu, W.; Huang, Y.; Kouri, D. J.; Chandler, C.; Hoffman, D. K. *Chem. Phys. Lett.* **1994**, *217*, 73.

(29) Mandelshtam, V. A.; Taylor, H. S. *J. Chem. Phys.* **1995**, *103*, 2903.
(30) Mandelshtam, V. A.; Taylor, H. S. *J. Chem. Phys.* **1995**, *102*, 7390.
(31) Chen, R.; Guo, H. *J. Chem. Phys.* **1996**, *105*, 1311.
(32) Chen, R.; Guo, H. *J. Chem. Phys.* **1996**, *105*, 3569.
(33) Gray, S. K.; Balint-Kurti, G. G. *J. Chem. Phys.* **1998**, *108*, 950.
(34) Chen, R.; Guo, H. *Comput. Phys. Commun.* **1999**, *119*, 19.
(35) Heller, E. J. *J. Chem. Phys.* **1978**, *68*, 2066.
(36) Guo, H. *J. Chem. Phys.* **1998**, *108*, 2466.
(37) Tannor, D. J.; Weeks, D. E. *J. Chem. Phys.* **1993**, *98*, 3884.
(38) Kouri, D. J.; Huang, Y.; Zhu, W.; Hoffman, D. K. *J. Chem. Phys.* **1994**, *100*, 3662.
(39) Wall, M. R.; Neuhauser, D. *J. Chem. Phys.* **1995**, *102*, 8011.
(40) Mandelshtam, V. A.; Taylor, H. S. *J. Chem. Phys.* **1997**, *106*, 5085.
(41) Xie, D.; Chen, R.; Guo, H. *J. Chem. Phys.* **2000**, *112*, 5263.
(42) Mandelshtam, V. A.; Carrington, T. *Phys. Rev.* **2002**, *E 65*, 028701.
(43) MOLPRO is a package of ab initio programs written by H.-J. Werner and P. J. Knowles with contributions from R. D. Amos et al.
(44) Werner, H.-J. *Adv. Chem. Phys.* **1987**, *LXIX*, 1.
(45) Dunning, T. H. *J. Chem. Phys.* **1989**, *90*, 1007.
(46) Light, J. C.; Carrington, T. *Adv. Chem. Phys.* **2000**, *114*, 263.
(47) Colbert, D. T.; Miller, W. H. *J. Chem. Phys.* **1992**, *96*, 1982.
(48) Kellman, M. E. *Annu. Rev. Phys. Chem.* **1995**, *46*, 395−421.
(49) Schinke, R. *Photodissociation Dynamics*;Cambridge University Press: Cambridge, U.K., 1993.